

Frequent homologous recombination deficiency in high-grade endometrial carcinomas.

Marthe M. de Jonge¹, Aurélie Auguste², Lise M. van Wijk³, Philip C. Schouten¹, Matty Meijers³, Natalja T. ter Haar¹, Vincent T.H.B.M. Smit¹, Remi A. Nout⁴, Mark A. Glaire⁵, David N. Church^{5,6}, Harry Vrieling³, Bastien Job⁷, Yannick Boursin², Cor D. de Kroon⁸, Etienne Rouleau⁹, Alexandra Leary^{2,10}, Maaïke P.G. Vreeswijk^{3*} and Tjalling Bosse^{1*}

*contributed equally

Department of ¹Pathology, ³Human Genetics, ⁴Radiotherapy, ⁸Gynecology, Leiden University Medical Center, Leiden, The Netherlands

Department of, ²INSERM U981, ⁷Plateforme de Bioinformatique, UMS AMMICA, ⁹Genetics, ¹⁰Medical Oncology, Gustave Roussy Cancer Center, Villejuif, France

⁵Wellcome Centre for Human Genetics, University of Oxford, Oxford, UK

⁶ National Institute for Health Research (NIHR) Oxford Biomedical Research Centre , Oxford University Hospitals NHS Foundation Trust, UK

Running Title: Homologous recombination deficiency in endometrial cancer.

Grant Support: The authors acknowledge grant support by The Dutch Cancer Society KWF-Alpe d'HuZes (grant EMCR: 2014-7048). MG is funded by a Wellcome Trust Clinical Training Fellowship. DC is funded by an Academy of Medical Sciences / Health Foundation Clinician Scientist Fellowship. This research was also funded by the National Institute for Health Research (NIHR) Oxford Biomedical Research Centre. The views expressed are those of the author(s) and not necessarily those of the NHS, the NIHR or the Department of Health

Disclosure of Potential Conflicts of Interest:

PCS's spouse is employed by AstraZeneca. No other potential conflicts of interest were disclosed.

Contact details Corresponding Author:

Tjalling Bosse

Leiden University Medical Center

Albinusdreef 2, 2333 ZA Leiden

E-mail: T.Bosse@lumc.nl

Phone: +31 071 526 6639

Fax: +31 071 52 66952

Word count manuscript text: 4750

Number of Tables: 1

Number of Figures: 5

Number of supplementary Tables: 3

Number of supplementary Figures: 2

Statement of translational relevance

The prognosis for women with high-grade endometrial cancers (EC) is poor, with little improvement in the last two decades. The mainstay of treatment is surgery (hysterectomy) with or without lymphadenectomy. While adjuvant radiotherapy is considered standard for high-risk EC, the added value of chemotherapy has been subject of recent trials. The randomised PORTEC-3 trial found a significant 5-year failure-free survival benefit (75.5% versus 68.6%, $P=0.022$) for women with high-risk EC treated with adjuvant chemotherapy both during and after radiotherapy versus radiotherapy alone. However, biomarkers predicting chemotherapeutic benefit for EC patients have not been defined to date. In this manuscript, we provide functional evidence that homologous recombination is frequently abrogated in a subset of EC, in particularly the “serous-like”, *TP53*-mutated subclass which have the worst clinical outcome. Our results suggest that homologous recombination deficiency holds promise as a marker to guide treatment decisions in high-risk EC, and supports prospective trials investigating agents such as platinum compounds and poly (ADP-ribose) polymerase (PARP) inhibitors to target this repair defect in these cancers.

Abstract:

Purpose The elevated levels of somatic copy number alterations (SCNA) in a subset of high-risk endometrial cancers (EC) are suggestive of defects in pathways governing genome integrity. We sought to assess the prevalence of homologous recombination deficiency (HRD) in EC and its association with histopathological and molecular characteristics.

Experimental Design Fresh tumor tissue was prospectively collected from 36 EC, and functional HRD was examined by the ability of replicating tumor cells to accumulate RAD51 protein at DNA double strand breaks (RAD51 foci) induced by ionizing radiation. Genomic alterations were determined by next generation sequencing and array comparative genomic hybridization/SNP array. The prevalence of *BRCA*-associated genomic scars—a surrogate marker for HRD—was determined in the TCGA EC cohort.

Results Most EC included in the final analysis (N=25) were of non-endometrioid (52%), grade 3 (60%) histology and FIGO-stage I (72%). HRD was observed in 24% (N=6) of cases and was restricted to non-endometrioid EC (NEEC), with 46% of NEEC being HRD compared to none of the endometrioid EC ($P=0.014$). All but one of the HRD cases harboured either a pathogenic *BRCA1* variant or high somatic copy number losses of HR genes. Analysis of TCGA cases supported these results, with *BRCA*-associated genomic scars present in up to 48% (63/132) of NEEC vs. 12% (37/312) of endometrioid EC ($P<0.001$).

Conclusions HRD occurs in EC, and is largely restricted to non-endometrioid, *TP53*-mutant EC. Evaluation of HRD may help select patients that could benefit from treatments targeting this defect, including platinum compounds and PARP inhibitors.

Introduction

Endometrial cancer (EC) is the most common gynaecological malignancy in developed countries (1), with surgery as its primary treatment modality. To guide adjuvant treatment, women with EC are stratified according to risk of recurrence using clinicopathologic characteristics (2,3). A heterogeneous group of 15-25% of ECs are currently considered at high-risk of disease recurrence. This group consists of patients with non-endometrioid endometrial carcinomas (NEEC) (uterine serous carcinoma (USC), uterine carcinosarcoma (UCS), clear cell carcinoma (CCC), undifferentiated carcinoma (UC), mixed EC), endometrioid EC (EEC) grade 3 stage IB-IV and EEC grade 1-2 stage II-IV (2-6). These patients have the poorest clinical outcome, despite optimum adjuvant treatment, which currently comprises a combination of pelvic radiotherapy with or without (platinum-taxane based) chemotherapy (3-5). In the cohort of Hamilton et al. high-risk EEC grade 3, USC and CCC represented only 28% of the total EC cohort but accounted for 74% of EC-related deaths (4), emphasizing the need for better systemic treatments to improve outcomes for these patients.

The Cancer Genome Atlas Research Network (TCGA) analysed EEC, USC and mixed carcinomas and identified four distinct molecular subclasses based on mutational load and somatic copy number alterations (SCNAs). These four subclasses are respectively the *POLE*/ultramutated (1), the microsatellite instability-high (MSI-high)/hypermuted (2), the SCNA low/no specific molecular profile (NSMP) (3) and the SCNA high (SCNA-hi)/serous-like EC (4)(7). Each of these has distinct risk of recurrence and clinical outcome, with *POLE*/ultramutated tumors showing excellent outcome and the SCNA-hi/serous-like subgroup showing the worst prognosis. The first three of these subclasses consist mainly of EEC with

variants in *PTEN* as the most frequent genetic alteration. In contrast, the SCNA-hi subclass almost exclusively comprises of USC and grade 3 EEC and is strongly associated with pathogenic variants in *TP53* (7). Interestingly, recent studies demonstrated that rare non-endometrioid subtypes, such as UCS, CCC and dedifferentiated carcinomas appear to be composed of the same four molecular subclasses, with UCS being mostly CNH/*TP53*-mutated and CCC, UC and dedifferentiated EC being more heterogeneous (8-11). The clinical relevance of these observations has increased by the recognition that the TCGA molecular subclasses of EC can be recapitulated using pragmatic surrogate markers resulting in subgroups with differing prognoses (12,13).

Another interesting observation of the TCGA study were the similarities between the SCNA spectra of the SCNA-hi/*TP53*-mutated EC subclass with those of high grade serous ovarian tubal carcinomas (HGSOCs) and basal-like breast cancers (7,8). Both HGSOC and basal-like breast cancer are part of the hereditary *BRCA1/2* related breast and ovarian cancer syndrome (HBOC syndrome) (14,15); characterised by failure of high-fidelity homologous recombination (HR) repair of DNA double-strand breaks (DSBs) mediated by *BRCA1* and *BRCA2* proteins (15,16). Although EC is not generally regarded as part of HBOC syndrome, case and cohort studies indicate that serous/serous-like ECs (including carcinosarcomas) are more prevalent in germline *BRCA1/2* mutation carriers than in the general population (17,18). Furthermore, germline alterations in other HR related genes have been described in EC patients (e.g. *ATM*, *BARD1*, *BRIP1*, *CHEK2*, *NBN*, *RAD51C*) (19), raising the question of whether a subset of ECs are HR-deficient. Shen et al. showed that *PTEN* has a role in the DSB-repair system by regulating the expression of *RAD51*, a key protein in HR-repair (20). Given the frequent somatic *PTEN* alterations

147 in EC, particularly in MMRd, *POLE* and NSMP-EC, it is conceivable that HR-
148 deficiency might also occur in these subclasses.

149 There are several methods to determine HR deficiency in tumors. Besides
150 sequencing of genes involved in HR, one can also assess the presence of specific
151 'genomic scars' caused by the use of alternative, error-prone pathways to repair
152 DSBs in the absence of HR. Examples of such alterations which are
153 overrepresented in *BRCA1/2*-null tumors include COSMIC Signature 3 and SCNA
154 profiles associated with widespread loss of heterozygosity (LOH), large-scale state
155 transitions (LST) and telomeric allelic imbalances (TAI) (16,21-24). A more direct
156 way of testing HR-capacity and one which more closely reflects the current status of
157 the tumor, is to determine the ability of tumor cells to perform HR in a functional
158 assay. For this, fresh viable tumor tissue is exposed *ex vivo* to ionizing radiation to
159 induce DNA DSBs. In HR-proficient tumor cells, RAD51 protein will be recruited to
160 these breaks leading to the formation of RAD51-containing ionizing radiation induced
161 foci (IRIF). In the case of HR-deficient tumor cells, RAD51-IRIF formation will be
162 impaired (16,25-27). The RAD51-assay, as a functional read out for HR, has been
163 shown to reliably identify cell lines, xenografts and fresh human tumor tissue with
164 defective HR (25-28).

165 The aim of this study was to assess the prevalence of HR-deficiency in EC using a
166 functional RAD51-IRIF assay, evaluate its association with clinicopathological
167 characteristics, and define the underlying molecular aetiology.

Material and Methods

Patient selection

Fresh EC tissue was obtained from patients who underwent surgery at the LUMC between August 2015 and January 2017. All patients with epithelial EC (including carcinosarcomas) were eligible for inclusion. After transportation of the surgical specimen to the pathology department, fresh tumor tissue was donated for research if sufficient tumor tissue was available. All cases obtained a unique research number and histotype was assigned by an experienced gynecopathologist (T.B.). The local medical ethics committee approved the study protocol (B16.019) and specimens were handled according to the “Code for Proper Secondary Use of Human Tissue in the Netherlands” (Dutch Federation of Medical Scientific Societies).

Functional Ex Vivo RAD51-assay to determine HR capacity

Fresh EC tissue samples were kept at 4°C in OSE culture medium (Wisent Bioproducts, cat. 316-030-CL) supplemented with 10% fetal bovine serum (FBS) and 1% penicillin-streptomycin (100 U/ml). Tissue was manually cut in 5-mm slices and after an incubation period of at least 4 hours at 37°C, the slice was irradiated with 5 Gy ionizing radiation (200kV, 4mA, YXLON Y.TU 225-D02) to induce DNA DSBs. Samples were then incubated on a rotating device (60 rpm) for two hours at 37°C in the OSE culture medium supplemented with 5-Ethynyl-2'-deoxyuridine (EdU) to a final concentration of 20µM (Component A) (cat. C10340, Click-iT® EdU Imaging Kits, invitrogen™) according to manufacturer's instructions. After incubation, tissue slices were fixed in formalin (4%) and embedded in paraffin. Left-over EC tissue was stored in liquid nitrogen in Recovery™ Cell Culture Freezing Medium (Sigma, cat. 12648010) to ensure viability after cryostorage.

Immunofluorescent staining

After irradiation and incubation, tumor samples were co-stained for RAD51, Geminin and EdU using anti-RAD51 (GTX70230, GeneTex), anti-geminin (10802-1-AP, Protein Tech group) and the Click-iT® reaction cocktail for EdU detection. For details, see Supplementary Methods.

Quality control and scoring of the RAD51-assay

To ensure high quality data we applied three stringent inclusion criteria. First, a semi-quantitative analysis of the quality of the tumor tissue was performed on a hematoxylin and eosin (H&E) stained serial section of the irradiated tumor slice used for the RAD51-IRIF assay. The tissue quality was scored (score 1-2=poor, 3-4=moderate, 5-6=good) based on the sum of the tissue vitality (1=poor, 2=moderate, 3=good) and tumor percentage (0=<5%, 1=5-20% 2=20-49% 3=≥50%). Samples were excluded when the total tissue quality score was two or less, or when the tumor percentage was <5%. Second, we only included samples for which we were able to score RAD51-IRIF in at least 50 geminin positive cells, defined by complete nuclear staining. Geminin is a cell-cycle marker to identify cells in the S/G₂-phase, the cell cycle phases in which HR is active. Third, >30% of the geminin positive cells had to be EdU positive. EdU is a nucleoside analogue that is actively incorporated into the DNA during DNA synthesis (29). Absence or low levels of EdU incorporation is indicative for limited DNA replication capacity of the tumor cells. As non-proliferative cells are not able to perform HR, this criterion avoids incorrect classification of tumors as HR-deficient. When one of these three criteria was not met, cryopreserved tissue from the same tumor was thawed, irradiated and analysed. If this “back-up” sample also failed to meet

all the quality controls, the tumor sample was excluded from further analysis.

For scoring, we used pre-established cut-off values (25). A tumor was considered HR-proficient when more than five RAD51-IRIF per nucleus were present in >50% of geminin positive cells and HR-deficient when $\leq 20\%$ of geminin-positive tumor cells formed RAD51-IRIF after ionizing radiation (Fig. 1). RAD51-IRIF formation in 21%-50% geminin positive tumor cells was considered HR-intermediate. All cases were scored for Geminin, RAD51 and EdU by two independent observers via immunofluorescence microscopy and the average score was used for the category assignment.

Genetic and epigenetic analyses

DNA isolation

Tumor DNA was isolated from formalin-fixed paraffin-embedded (FFPE) tissue blocks either by taking three 0.6 mm tumor cores or by microdissection of tumor areas (10 μm slides). DNA isolation was performed fully automated using the Tissue Preparation System (Siemens Healthcare Diagnostics) as described previously (30). Additionally, for a subset of cases, high quality tumor DNA was isolated from frozen tumor tissue using 5-10 whole cryosections (20 μm) and the Wizard® Genomic DNA purification KIT (Promega) according to manufacturer's protocol. An H&E cryoslide (5 μm) was made to determine tumor percentage. The Qubit™ dsDNA HS Assay Kit was used for DNA quantification according to manufacturer's instructions (Qubit 2.0 Fluorometer, Life Technologies, Carlsbad, CA).

aCGH / SNP array to determine somatic copy number alterations

Somatic copy number alterations were determined using either the Agilent SurePrint G3 CGH Microarray (8 x 60k probes, Agilent technologies) on 300ng DNA derived from frozen tumor tissue (n=16, Case-ID; 1, 3, 6, 7, 9, 12, 13, 14, 15, 16, 17, 18, 19, 21, 22, 24) or the OncoScan™ FFPE Assay Kit (335k probes, Thermo Fisher) on 80ng FFPE-isolated DNA (n=9, Case-ID; 20, 25, 26, 27, 29, 32, 33, 34, 36). Prior paired analysis of ten ovarian tumor samples showed that the SCNA were similar independently of the platform used (Supplementary Figure S1). Furthermore, unsupervised Pearson hierarchical clustering performed on the included tumor samples demonstrated a natural division between samples independent of the platform used (Supplementary Figure S2). For both platforms, samples were included when the tumor cell percentage was at least 30%. The mean tumor cell percentage of the DNA derived from frozen tumor tissue samples included for the aCGH was 78% (range: 30-95%). The mean tumor cell percentage of the FFPE-tissue isolated DNA samples for the SNP array was 71% (range: 50-90%). Analysis was performed according to manufacturer's instructions. Microarray data is available upon request. For details, see Supplementary Methods.

Genomic Instability Score

The genomic instability score (GIS) was calculated as the number of altered segments superior to 15Mbp and inferior to chromosome arm, and samples were classified in three categories using an unsupervised machine learning (kmeans – python scikit) based on GIS. For details on the analysis, see supplementary methods. The three categories were somatic copy number alteration low (SCNA-low), somatic copy number alteration high (SCNA-high) and somatic copy number alteration extremely high (SCNA-extremely high).

Somatic Copy Number Losses

As a marker for potential loss of function of HR genes, the presence of “high somatic copy number (SCN) losses” was determined for all cases by using a very stringent cut-off value; $\log_2\text{ratio} \leq -0.7$. This stringent cut-off value was used to select for SCN losses in genes that are more likely clonal and/or homozygous. The same cut-off was applied for both platforms (CGH Agilent and Oncoscan) as both yield similar results. HR genes were defined according to a previously published list by Riaz et al. HR-genes were categorized as either “core” HR genes (involved in the core HR machinery) or “related” HR genes (involved in closely related processes) (31).

Next generation sequencing (NGS)

NGS was performed using FFPE-isolated tumor DNA with a total input of 500-1000ng per sample. The mean tumor cell percentage of the included samples was 68% (range: 30%-90%). An Agilent Sureselect^{XT} HS Custom panel made in SureDesign (Agilent technologies, Santa Clara, California, United States) was used for variant detection with the following HR-genes design: *ATM*; exons 2-63, *BARD1*; exons 1-10, *BRCA1*; exons 1-24, *BRCA2*; exons 2-27, *BRIP1*; exons 2-20, *CDK12*; exons 1-14, *CHEK2*; exons 2-15, *PALB2*; exons 1-13, *RAD51C*; exons 1-9, *RAD51D*; exons 1-14. Additional genes included in the panel were *TP53* (exons 1-12) and *CCNE1* (only for amplification detection). For details on the data analysis, see Supplementary Methods.

Variants were categorized using the five-tier pathogenicity classification according to Plon et al., 2008; class 1=benign, class 2=likely benign, class 3=variant of unknown significance (VUS), class 4=likely pathogenic, class 5=pathogenic (32). Only class 3, 4 and 5 variants are reported in the manuscript. Variants were annotated based on

291 build GRCH37 (hg19) using the following transcript numbers: *ATM*; NM_000051.3,
292 *BRCA1*; NM_007294.3, *BRCA2*; NM_000059.3, *BRIP1*; NM_032043.2, *CHEK2*;
293 NM_007194.3, *CDK12*; NM_016507.3, *RAD51D*; NM_002878.3.

294 *BRCA1* hypermethylation using MS-MLPA

295 The presence of *BRCA1* promotor hypermethylation was assessed for all cases
296 using tumor DNA isolated from FFPE-tissue. For this, the SALSA® MLPA® ME001
297 was used as described in the Supplementary Methods.

298 *Immunohistochemical (IHC) analysis*

299 If not yet performed in routine diagnostics (Autostainer Link 48, DAKO), additional
300 IHC-stainings for PMS2 (Clone EP51, 1:25, DAKO), MSH6 (Clone EPR3945, 1:400,
301 GeneTex), PTEN (Clone 6H2.1, 1:200, DAKO), MRE11 (clone 31H4, 1:400, cell
302 signalling) and BAP1 (Clone C4, 1:100, Santa Cruz) were performed on whole slides
303 (4 µm) as described in the Supplementary Methods.

304 *POLE* sequencing

305 Uni-directional Sanger sequencing was performed to screen exons 9 (forward), 13
306 (reverse) and 14 (reverse) for somatic *POLE* exonuclease domain mutations as
307 previously described using FFPE tumor DNA (33). To sequence exon 14, the
308 following primers were used; forward: 5'- tctggcgttctctcctcag-3', reverse: 5'-
309 cgacaggacagataatgctcac-3'. Mutations were confirmed by Sanger sequencing in the
310 opposite direction. *POLE* transcript NM_006231.3 was used for variant annotation.

311 *TCGA classification based on surrogate markers*

All ECs included in this study were classified according to the previously described molecular subclasses using a surrogate marker approach. For details, see Supplementary Methods.

***BRCA*-associated genomic scars in the TCGA cohort**

To determine the presence of *BRCA*-associated genomic scars in the TCGA-EC cohort, SCNA data and somatic mutation annotation files (MAF) were obtained from Firebrowse (<http://firebrowse.org/>) using data version 2016_01_28; doi:10.7908/C11G0KM9 (34). First, we assessed the presence of specific patterns of somatic copy-number gains and losses that have previously been linked to *BRCA1* or *BRCA2* mutated breast and ovarian cancer to classify tumors in *BRCA*-like or non-*BRCA*-like (35). Second, we assessed the number of LST, the presence of COSMIC signature 3 and the presence of bi-allelic pathogenic mutations in 102 HR genes as defined by Riaz and colleagues (31). For details regarding these analyses, see Supplementary Methods.

Statistics

Comparison of age between groups was performed using the unpaired t-test. Associations between all categorical variables were tested using a 2-sided Fisher's exact test. A *P*-value of <0,05 was considered significant. Cohen's kappa coefficient (κ) was used to measure interobserver and intertest agreement. IBM SPSS version 23.0 (SPSS, Inc., Chicago, USA) and R (<http://r-project.org>) were used for statistical analysis.

Results

Homologous recombination repair deficiency and clinicopathologic characteristics

Fresh tumor tissue was prospectively obtained from 36 patients. Twenty-five samples (12 EEC and 13 NEEC) passed our stringent quality controls and were included for further analyses (Fig. 2). Clinicopathological characteristics of the total cohort are described in Supplementary Table S1. The percentage of Geminin+/RAD51+ cells scored after *ex vivo* exposure to ionizing radiation by the two independent observers was comparable, with a median score difference within cases of 6% (range; 0%-41%). Interrogator reliability for final HR category assignment was high ($\kappa=0.85$).

In total, six (24%) EC were classified as HR-deficient, 17 (68%) as HR-proficient and two (8%) as HR-intermediate. Clinicopathological characteristics of groups stratified by HR status are shown in Table 1 and Fig. 3A. HR-intermediate cases are described in Supplementary Table S2. HR deficiency was significantly associated with non-endometrioid histology; all six (100%) HR-deficient tumors were NEEC, compared to none of 12 EEC tested ($P=0.014$). The six HR-deficient NEEC were either USC ($n=3$, 50%) or UCS with serous epithelial component ($n=3$, 50%). The 17 HR-proficient tumors were histologically more diverse; 11 (65%) EEC, two (12%) CCC, two (12%) dedifferentiated carcinomas, one (6%) USC and one (6%) UCS with serous epithelial component. When only considering USC and UCS (both with serous and endometrioid epithelial component), six out of nine tumors (67%) were HR-deficient.

HR-deficient EC were more often high grade (grade 3) (100%) compared to HR-proficient EC (41%, $P=0.019$), reflecting the non-endometrioid histology in the HR-

deficient group. HR-deficient EC presented more often in a high FIGO-stage compared to HR-proficient EC (I versus III/IV; $P=0.021$) and had more frequent lymph-vascular space involvement ($P=0.045$). We did not observe an association between HR-deficiency and loss of PTEN expression by IHC, with one (17%) of the HR-deficient cases showing PTEN loss compared to 47% of HR-proficient cases ($P=0.340$). There was also no association between HR capacity and age of EC diagnosis ($P=0.431$). *TP53* variants were more often present in HR-deficient tumors (100%) compared to HR-proficient tumors (41%) ($P=0.019$). In total, 46% of the *TP53*-mutated EC were HR-deficient.

Two cases were assigned HR-intermediate. One was a grade 3 EEC that was just above the threshold of being HR-deficient (Case 27; Geminin+/RAD51+; 23%). The other case was a UCS with an endometrioid epithelial component (Case 18; Geminin+/RAD51+; 44%, Fig. 3A and Supplementary Table S2).

Homologous recombination repair capacity and molecular subgroups

Surrogate markers were used to classify the EC into the four molecular subgroups as defined by the TCGA study (Table 1, Fig. 3A). HR-deficient EC were significantly more often classified as SCNA-hi/*TP53*-mutated compared to HR-proficient EC, with all HR-deficient EC being SCNA-hi/*TP53*-mutated compared to six (35%) of the HR-proficient EC ($P=0.014$). The HR-proficient group was heterogeneous with all molecular subgroups represented; nine (53%) NSMP, six (35%) SCNA-hi/*TP53*-mutated, one (6%) *POLE*/ultramutated and one (6%) MMRd/hypermuted.

To further characterise our cohort, we performed SCNA analyses using a genomic instability score based on the number of altered segments greater than 15Mbp and smaller than a whole chromosome arm (GIS). For this, samples were classified in

three categories using unsupervised machine learning (k-means clustering); SCNA-low, SCNA-high and SCNA-extremely high. All HR-deficient EC (100%) were either SCNA-high (n=2) or SCNA-extremely high (n=4), compared to seven (41%; 6 SCNA-high, 1 SCNA-extremely high) of the HR-proficient EC ($P=0.019$, Fig. 3A and Table 1). An association was observed between the SCNA status and the presence of a *TP53* variant, with *TP53* variants being significantly more common in SCNA-high or extremely high EC (11/14 (79%)) compared to SCNA-low EC (2/11 (18%), $P=0.005$).

Genetic alterations in HR genes and relation to HR phenotype

We performed (epi)genetic analysis to identify possible loss of function alterations that could explain the HR deficiency. This included NGS (variants HR genes), aCGH/SNP array (high SCN losses of HR genes; $\log_2\text{Ratio} \leq -0.7$), MS-MLPA (*BRCA1* promoter hypermethylation) and immunohistochemistry (MRE11, BAP1).

In two out of six HR-deficient EC the presence of a pathogenic *BRCA1* variant with loss of heterozygosity (LOH) of the wildtype allele could explain the HR-deficient phenotype (case 9; *BRCA1*, c.4327C>T, p.Arg1443* and case 15; *BRCA1*, c.3013delG, p.Glu1005fs), see Fig. 3B and Supplementary Table S3. Two other HR-deficient cases harboured a VUS in an HR gene; Case 36; *RAD51D*, c.433C>T, p.Arg145Cys and case 19; *ATM*, c.6543G>T, p.Glu2181Asp. As it is uncertain whether these variants will affect protein function and the variant allele frequency (VAF) was low (respectively 32%, and 34%) with tumor percentages of respectively 75% and 70%, it is unlikely that these variants were causative for the observed HR-deficiency.

404 High SCN losses in HR core and HR related genes were observed for both cases in
405 which no variants were identified (case 12 and 13) and for case 19 in which a VUS in
406 *ATM* was detected (Fig. 3B and Fig. 4). Case 36, in which a *RAD51D* VUS was
407 identified, did not show SCN losses in HR genes with a log2ratio of ≤ -0.7 . None of
408 the included cases demonstrated *BRCA1* promoter hypermethylation or
409 immunohistochemical BAP1 or MRE11 expression loss.

410 In the HR-proficient EC, variants in HR genes were present in two cases (Fig. 3B).
411 Case 26, the *POLE*-mutated tumor, harboured a class 5 *CHEK2* variant c.1510G>T,
412 p.Glu504* (VAF: 28%) that likely occurred as a consequence of the *POLE* mutation
413 as it is concordant with the known mutational bias it causes (36). Case 23, the
414 MMRd EC, harboured four *ATM* variants. One of the four *ATM* variants was a class 5
415 variant; c.640delT, p.Ser214fs, VAF: 5,5%, the remaining three were all VUS
416 (Supplementary Table S3). None of the HR-proficient EC demonstrated high SCN
417 losses of the HR core genes. Case 01 and Case 34 did show high SCN losses in HR
418 related genes (Fig. 3B and Fig.4).

419 Two EC demonstrated an HR-intermediate phenotype (Fig. 3A and B,
420 Supplementary Table S2). Case 27 harboured two *BRCA2*, one *BRIP1* and one
421 *CDK12* variant. The *BRCA2* variant with the highest VAF (64%) was a duplication of
422 an adenine; c.6373dupA , p.Thr2125fs. Additionally, an in-frame deletion
423 (c.6306_6413del, p.Ser2103_Val2138del) spanning the frameshift variant was
424 present with a VAF of 28%, likely restoring the *BRCA2* function in a subset of the
425 tumor cells. Case 18 harboured a class 5 *BRIP1* variant; c.632delC, p.Pro211fs with
426 a VAF of 28%. None of the HR-intermediate cases demonstrated high SCN losses in
427 the HR core genes. Case 27 did show SCN losses in one HR related gene (Fig. 3B
428 and Fig. 4).

***BRCA*-associated genomic scars in the TCGA cohort**

To validate the occurrence of HR deficiency in an additional EC cohort, we used SCNA data and somatic mutation annotation files (MAF) from the TCGA study to determine the presence of *BRCA*-like profiles (data available for N=536), Large-Scale State Transitions (data available for N=444), COSMIC signature 3 (data available for N=246) and pathogenic bi-allelic alterations in HR genes (data available for N=541). Since our data showed a clear difference in the presence of HR-deficiency between EEC and non-endometrioid EC, we stratified the cohort by histotype (EEC versus NEEC, the latter including both mixed-EC and USC). Both a *BRCA*-like profile and a high LST-score were significantly more common in NEEC (*BRCA*-like profile: 41.2%, LST; 47.7%) compared to the EEC (*BRCA*-like profile; 8.0%, LST; 11.9%), $P<0.001$ (Fig. 5A and 5B). COSMIC signature 3 was present in 6.6% of EEC and 45.8% of NEEC ($P<0.001$, Figure 5C). It was present as dominant signature in 1.0% (N=2) of EEC and 6.3% of NEEC (N=3, $P=0.052$). Somatic or germline pathogenic bi-allelic variants in HR pathway genes were present in 4.4% of EEC and in 1.5% NEEC ($P=0.19$, Figure 5D). The high prevalence of *BRCA*-associated genomic scars in the TCGA-EC cohort supports that HR-deficiency occurs in EC, especially in NEEC, as observed in our prospective cohort.

Discussion:

Using a functional assay to assess homologous recombination repair capacity, we found that HR-deficiency is common in EC, especially in NEEC (46%). The observation that all HR-deficient EC were *TP53*-mutated and of USC or UCS histology (comprising 67% of the included USC/UCS), further extends the established parallels between a subset of EC and HGSOC. In five out of six HR-deficient tumors, we identified alterations in core HR genes (two cases with a pathogenic variant in *BRCA1* and three cases with high somatic copy number losses of HR core genes). Independent validation using the TCGA EC cases in which we determined the prevalence of *BRCA*-associated genomic scars underscored the high prevalence of HR-deficiency in NEEC.

Using established cut-off values to assign EC to different HR categories, we were able to assign 23/25 EC into either the HR-deficient or HR-proficient category, leaving two cases in the HR-intermediate category (case 27 and 18). Case 27 was a second recurrence of a *TP53*-wildtype grade 3 EEC after two previous lines of platinum-based chemotherapy. At initial treatment there was a partial response (according to the RECIST-criteria) after 3 courses of neo-adjuvant carboplatin/paclitaxel. Genomic analysis identified two *BRCA2* variants; one truncating frameshift variant and one in-frame deletion spanning the region containing the frameshift variant. It is likely that the in-frame deletion is a secondary somatic variant (partially) restoring the *BRCA2* function, a scenario described previously (37). This is a relevant observation, as it suggests that *TP53*-wildtype EC with endometrioid histology may also be HR-deficient.

PTEN alterations are frequent in EC, particularly in EEC and may modulate DSB-repair capacity by regulating the expression of RAD51 (20). *In vitro* studies have

shown contradictory results, with some reporting no correlation between PTEN loss and HR-deficiency (38,39) whilst others did find a correlation (40). In our study, we did not observe a correlation between HR capacity and immunohistochemical PTEN expression.

Based on the high prevalence of HR-deficiency in our cohort, one might speculate that a proportion of, especially the serous/serous-like EC would be responsive to platinum-based chemotherapy (41,42). The PORTEC-3 trial suggested that the addition of platinum/taxane-based chemotherapy to radiotherapy in USC patients resulted in a similar failure-free survival benefit as for the overall cohort of high-risk EC patients, although this benefit was not significant (43). Furthermore, a grouped analysis among 1203 patients with advanced or recurrent EC participating in four Gynecologic Oncology Groups (GOG) trials found similar overall response rates to chemotherapy for USC as for other histotypes (EEC, CCC) (44). In contrast, the pooled analysis of the NSGO-EC-9501/EORTC-55991 trials showed a significant progression-free survival benefit of the addition of adjuvant (platinum-based) chemotherapy for EEC but not USC and CCC patients (45). Possible explanations for these different trial outcomes may be the small number of included USC, the different chemotherapy combinations used within trials (apart from PORTEC-3) and finally, the major difficulties pathologists are having with assigning histotype, particularly in high-grade EC (46). For these reasons, future EC trial-designs in which (platinum-based) chemotherapy is included, should consider HR-status as a biomarker for treatment stratification.

Multiple studies have already shown that PARP-inhibitors improve progression-free survival (PFS) in patients with platinum sensitive recurrent ovarian cancer (47-49).

Although most treatment benefit is observed for *BRCA1/2* mutated tumors, an

increased beneficial effect could also be observed for tumors with genetic alterations that are suggestive for HR-deficiency as assessed by “genomic scar” assays (47-49). Our results suggests PARP inhibitors as a potential new treatment modality for the HR-deficient subgroup of EC, which is further supported by a recently published case report in which an EEC-patient with a germline *BRCA2* variant (and a somatic hit of wildtype allele) experienced a durable response to the PARP inhibitor olaparib (50).

The performance of several candidate “HRD-biomarkers” to predict therapy response are currently being studied, among which many that include the analysis of pathogenic variants in HR-genes or the presence of *BRCA* associated “genomic scars” in tumor DNA (16,21-23,51). At this moment, it is still unknown which of the available HRD biomarkers is most powerful to predict therapy response. The HR status as determined by the RAD51-assay used in this study, has been shown to be strongly associated with achieving a complete pathological response to neoadjuvant chemotherapy in breast cancer patients (26), could predict in vitro PARP-inhibitor cytotoxicity in primary cell cultures obtained from epithelial ovarian cancers (52,53) and could predict platinum sensitivity as well as improved survival outcome in EOC and HGSOC patients (27,53). Since the RAD51-assay is performed on fresh, irradiated tumor tissue, it currently has limited potential to be routinely used in clinical diagnostics, whereas methods that can assess “genomic scars” in FFPE-derived DNA are more suitable for this purpose (51). Interestingly, in the recently published study of Cruz et al. low levels of RAD51 foci in non-irradiated tumors correlated with PARP-inhibitor sensitivity in xenograft models (54). When this approach can be validated on (archived) human FFPE-tumor tissue, the assessment of RAD51 to define HR status would become clinically feasible.

Our study is not without limitations. Our cohort is enriched for high-grade EC cases, since we prospectively recruited patients in the LUMC (The Netherlands), which is a referral centre for EC. Therefore, the prevalence of HR-deficiency in our EC cohort is likely an overestimate given the strong association with NEEC. Studies on larger cohorts are necessary to establish a more precise estimate of the prevalence of HR-deficiency among the diverse EC histotypes. Finally, the molecular analysis we performed was extensive, but not exhaustive. We used a targeted NGS panel and a aCGH/SNP array to identify the molecular cause of HR deficiency. In the future, whole exome/genome sequencing may be preferred, not only to have the possibility to identify pathogenic variants in additional genes but also to explore the relationship between the outcome of the RAD51-assay and established genomic scars.

In conclusion, we are the first to demonstrate that HR is frequently abrogated in a subset of EC, in particularly the “serous-like”, *TP53*-mutated subclass of EC, the group with the worst clinical outcome. This study provides a strong rationale for future clinical trials aiming to target HR-deficient high-grade EC with therapies exploiting this defect, such as platinum compounds and PARP inhibitors.

Authors' Contributions

Conception and design: T. Bosse, M.P.G. Vreeswijk, H. Vrieling, V.T.H.B.M. Smit, A. Leary, C.D. de Kroon, M.M. de Jonge, A. Auguste

Development of methodology: T. Bosse, M.P.G. Vreeswijk, H. Vrieling, A. Leary, E. Rouleau, B. Job, Y. Boursin, P.C. Schouten, M.M. de Jonge, A. Auguste, N.T. ter Haar

Acquisition of data (provided animals, acquired and managed patients, provided facilities, etc.): M.M. de Jonge, A. Auguste, P.C. Schouten, L.M. van Wijk, Y. Boursin, M. Meijers, M. Glaire, D.N. Church, N.T. ter Haar, C.D. de Kroon, E. Rouleau, A. Leary, M.P.G. Vreeswijk, T. Bosse

Analysis and interpretation of data (e.g., statistical analysis, biostatistics, computational analysis): M.M. de Jonge, A. Auguste, P.C. Schouten, L.M. van Wijk, M. Meijers, N.T. ter Haar, V.T.H.B.M. Smit, R.A. Nout, M. Glaire, D.N. Church, B. Job, Y. Boursin, C.D. de Kroon, E. Rouleau, A. Leary, M.P.G. Vreeswijk, T. Bosse

Writing, review, and/or revision of the manuscript: M.M. de Jonge, A. Auguste, L.M. van Wijk, P.C. Schouten, B. Job, Y. Boursin, N.T. ter Haar, R.A. Nout, V.T.H.B.M. Smit, H. Vrieling, M. Glaire, D.N. Church, C.D. de Kroon, E. Rouleau, A. Leary, M.P.G. Vreeswijk, T. Bosse

Administrative, technical, or material support (i.e., reporting or organizing data, constructing databases): M.M. de Jonge, A. Auguste, L.M. van Wijk, P.C. Schouten, M. Meijers, N.T. ter Haar, B. Job, Y. Boursin, E. Rouleau, M.P.G. Vreeswijk, T. Bosse

Study supervision: V.T.H.B.M. Smit, C.D. de Kroon, Y. Boursin, E. Rouleau, A. Leary, M.P.G. Vreeswijk, T. Bosse

Acknowledgements

The authors would thank E.M. Osse (LUMC), E.J. Dreef (LUMC), M. Francillette (IGR), for their excellent technical assistance.

571 References

- 572 1. Torre LA, Bray F, Siegel RL, Ferlay J, Lortet-Tieulent J, Jemal A. Global cancer
573 statistics, 2012. *CA Cancer J Clin* **2015**;65(2):87-108.
- 574 2. Colombo N, Creutzberg C, Querleu D, Barahona M, Sessa C, ESMO Guidelines
575 Committee. Appendix 5: Endometrial cancer: eUpdate published online 8 June 2017
576 (www.esmo.org/Guidelines/Gynaecological-Cancers). *Ann Oncol*
577 **2017**;28(suppl_4):iv153-iv6.
- 578 3. Colombo N, Creutzberg C, Amant F, Bosse T, Gonzalez-Martin A, Ledermann J, *et al.*
579 ESMO-ESGO-ESTRO Consensus Conference on Endometrial Cancer: Diagnosis,
580 Treatment and Follow-up. *Int J Gynecol Cancer* **2016**;26(1):2-30.
- 581 4. Hamilton CA, Cheung MK, Osann K, Chen L, Teng NN, Longacre TA, *et al.* Uterine
582 papillary serous and clear cell carcinomas predict for poorer survival compared to
583 grade 3 endometrioid corpus cancers. *Br J Cancer* **2006**;94(5):642-6.
- 584 5. McGunigal M, Liu J, Kalir T, Chadha M, Gupta V. Survival Differences Among
585 Uterine Papillary Serous, Clear Cell and Grade 3 Endometrioid Adenocarcinoma
586 Endometrial Cancers: A National Cancer Database Analysis. *Int J Gynecol Cancer*
587 **2017**;27(1):85-92.
- 588 6. Bendifallah S, Canlorbe G, Collinet P, Arsene E, Huguet F, Coutant C, *et al.* Just how
589 accurate are the major risk stratification systems for early-stage endometrial cancer?
590 *Br J Cancer* **2015**;112(5):793-801.
- 591 7. Kandoth C, Schultz N, Cherniack AD, Akbani R, Liu Y, Shen H, *et al.* Integrated
592 genomic characterization of endometrial carcinoma. *Nature* **2013**;497(7447):67-73.
- 593 8. Cherniack AD, Shen H, Walter V, Stewart C, Murray BA, Bowlby R, *et al.* Integrated
594 Molecular Characterization of Uterine Carcinosarcoma. *Cancer cell* **2017**;31(3):411-
595 23.
- 596 9. Rosa-Rosa JM, Leskela S, Cristobal-Lana E, Santon A, Lopez-Garcia MA, Munoz G,
597 *et al.* Molecular genetic heterogeneity in undifferentiated endometrial carcinomas.
598 *Mod Pathol* **2016**;Nov;29(11):1390-1398.
- 599 10. DeLair DF, Burke KA, Selenica P, Lim RS, Scott SN, Middha S, *et al.* The genetic
600 landscape of endometrial clear cell carcinomas. *J Pathol.* **2017**;243(2):230-241.
- 601 11. Stelloo E, Bosse T, Nout RA, MacKay HJ, Church DN, Nijman HW, *et al.* Refining
602 prognosis and identifying targetable pathways for high-risk endometrial cancer; a
603 TransPORTEC initiative. *Mod Pathol* **2015**;28(6):836-44.
- 604 12. Talhouk A, McConechy MK, Leung S, Li-Chang HH, Kwon JS, Melnyk N, *et al.* A
605 clinically applicable molecular-based classification for endometrial cancers. *Br J*
606 *Cancer* **2015**;113(2):299-310.
- 607 13. Stelloo E, Nout RA, Osse EM, Jurgenliemk-Schulz IJ, Jobsen JJ, Lutgens LC, *et al.*
608 Improved Risk Assessment by Integrating Molecular and Clinicopathological Factors
609 in Early-stage Endometrial Cancer-Combined Analysis of the PORTEC Cohorts. *Clin*
610 *Cancer Res* **2016**;22(16):4215-24.
- 611 14. Konstantinopoulos PA, Ceccaldi R, Shapiro GI, D'Andrea AD. Homologous
612 Recombination Deficiency: Exploiting the Fundamental Vulnerability of Ovarian
613 Cancer. *Cancer Discov* **2015**;5(11):1137-54.
- 614 15. Lord CJ, Ashworth A. BRCAness revisited. *Nat rev Cancer* **2016**;16(2):110-20.
- 615 16. Roy R, Chun J, Powell SN. BRCA1 and BRCA2: different roles in a common pathway
616 of genome protection. *Nat Rev Cancer* **2012**;12(1):68-78.
- 617 17. de Jonge MM, Mooyaart AL, Vreeswijk MP, de Kroon CD, van Wezel T, van Asperen
618 CJ, *et al.* Linking uterine serous carcinoma to BRCA1/2-associated cancer
619 syndrome: A meta-analysis and case report. *Eur J Cancer* **2017**;72:215-25.
- 620 18. Shu CA, Pike MC, Jotwani AR, Friebel TM, Soslow RA, Levine DA, *et al.* Uterine
621 Cancer After Risk-Reducing Salpingo-oophorectomy Without Hysterectomy in
622 Women With BRCA Mutations. *JAMA oncol* **2016**; 1;2(11):1434-1440.

19. Ring KL, Bruegl AS, Allen BA, Elkin EP, Singh N, Hartman AR, *et al.* Germline multi-gene hereditary cancer panel testing in an unselected endometrial cancer cohort. *Mod Pathol* **2016** Nov;29(11):1381-1389.
20. Shen WH, Balajee AS, Wang J, Wu H, Eng C, Pandolfi PP, *et al.* Essential role for nuclear PTEN in maintaining chromosomal integrity. *Cell* **2007**;128(1):157-70.
21. Davies H, Glodzik D, Morganella S, Yates LR, Staaf J, Zou X, *et al.* HRDetect is a predictor of BRCA1 and BRCA2 deficiency based on mutational signatures. *Nat Med* **2017**;23(4):517-525.
22. Abkevich V, Timms KM, Hennessy BT, Potter J, Carey MS, Meyer LA, *et al.* Patterns of genomic loss of heterozygosity predict homologous recombination repair defects in epithelial ovarian cancer. *Br J Cancer* **2012**;107(10):1776-82.
23. Popova T, Manie E, Rieunier G, Caux-Moncoutier V, Tirapo C, Dubois T, *et al.* Ploidy and large-scale genomic instability consistently identify basal-like breast carcinomas with BRCA1/2 inactivation. *Cancer Res* **2012**;72(21):5454-62.
24. Alexandrov LB, Nik-Zainal S, Wedge DC, Aparicio SA, Behjati S, Biankin AV, *et al.* Signatures of mutational processes in human cancer. *Nature* **2013**;500(7463):415-21.
25. Naipal KA, Verkaik NS, Ameziane N, van Deurzen CH, Ter Brugge P, Meijers M, *et al.* Functional ex vivo assay to select homologous recombination-deficient breast tumors for PARP inhibitor treatment. *Clin Cancer Res* **2014**;20(18):4816-26.
26. Graeser M, McCarthy A, Lord CJ, Savage K, Hills M, Salter J, *et al.* A marker of homologous recombination predicts pathologic complete response to neoadjuvant chemotherapy in primary breast cancer. *Clin Cancer Res* **2010**;16(24):6159-68.
27. Tumiati M, Hietanen S, Hynninen J, Pietila E, Farkkila A, Kaipio K, *et al.* A functional homologous recombination assay predicts primary chemotherapy response and long-term survival in ovarian cancer patients. *Clin Cancer Res* **2018** 24(18):4482-4493.
28. Willers H, Taghian AG, Luo CM, Treszezamsky A, Sgroi DC, Powell SN. Utility of DNA repair protein foci for the detection of putative BRCA1 pathway defects in breast cancer biopsies. *Mol Cancer Res* **2009**;7(8):1304-9.
29. Buck SB, Bradford J, Gee KR, Agnew BJ, Clarke ST, Salic A. Detection of S-phase cell cycle progression using 5-ethynyl-2'-deoxyuridine incorporation with click chemistry, an alternative to using 5-bromo-2'-deoxyuridine antibodies. *BioTechniques* **2008**;44(7):927-9.
30. van Eijk R, Stevens L, Morreau H, van Wezel T. Assessment of a fully automated high-throughput DNA extraction method from formalin-fixed, paraffin-embedded tissue for KRAS, and BRAF somatic mutation analysis. *Exp Mol Pathol* **2013**;94(1):121-5.
31. Riaz N, Blecua P, Lim RS, Shen R, Higginson DS, Weinhold N, *et al.* Pan-cancer analysis of bi-allelic alterations in homologous recombination DNA repair genes. *Nat Commun* **2017**;8(1):857.
32. Plon SE, Eccles DM, Easton D, Foulkes WD, Genuardi M, Greenblatt MS, *et al.* Sequence variant classification and reporting: recommendations for improving the interpretation of cancer susceptibility genetic test results. *Hum Mutat* **2008**;29(11):1282-91.
33. Church DN, Stelloo E, Nout RA, Valtcheva N, Depreeuw J, ter Haar N, *et al.* Prognostic significance of POLE proofreading mutations in endometrial cancer. *J Natl Cancer Inst* **2015**;107(1):402.
34. Broad Institute TCGA Genome Data Analysis Center (2016): Firehose 2016_01_28 run. Broad Institute of MIT and Harvard. doi:10.7908/C11G0KM9.
35. Schouten PC, Vis DJ, van Dijk E, Lips EH, Scheerman E, van Deurzen CHM, *et al.* Chapter 3: Copy number signatures of *BRCA1* and *BRCA2* association across breast and ovarian cancer. In: Schouten P.C. Identification and treatment of patients with *BRCA1* or *BRCA2*-defective breast and ovarian cancer. Genes and mechanisms involved in malignant conversion. In: Harris CC, Liotta LA, editors. Genetic

- mechanisms in carcinogenesis and tumor progression. ProefschriftMaken; 2016 p. 95-132.
36. Rayner E, van Gool IC, Palles C, Kearsey SE, Bosse T, Tomlinson I, *et al.* A panoply of errors: polymerase proofreading domain mutations in cancer. *Nat Rev Cancer* **2016**;16(2):71-81.
 37. Norquist B, Wurz KA, Pennil CC, Garcia R, Gross J, Sakai W, *et al.* Secondary somatic mutations restoring BRCA1/2 predict chemotherapy resistance in hereditary ovarian carcinomas. *J Clin Oncol* **2011**;29(22):3008-15.
 38. Bian X, Gao J, Luo F, Rui C, Zheng T, Wang D, *et al.* PTEN deficiency sensitizes endometrioid endometrial cancer to compound PARP-PI3K inhibition but not PARP inhibition as monotherapy. *Oncogene* **2018**;37(3):341-51.
 39. Miyasaka A, Oda K, Ikeda Y, Wada-Hiraike O, Kashiwayama T, Enomoto A, *et al.* Anti-tumor activity of olaparib, a poly (ADP-ribose) polymerase (PARP) inhibitor, in cultured endometrial carcinoma cells. *BMC cancer* **2014**;14:179.
 40. Mendes-Pereira AM, Martin SA, Brough R, McCarthy A, Taylor JR, Kim JS, *et al.* Synthetic lethal targeting of PTEN mutant cells with PARP inhibitors. *EMBO Mol Med* **2009**;1(6-7):315-22.
 41. Vollebergh MA, Lips EH, Nederlof PM, Wessels LF, Wesseling J, Vd Vijver MJ, *et al.* Genomic patterns resembling BRCA1- and BRCA2-mutated breast cancers predict benefit of intensified carboplatin-based chemotherapy. *Breast cancer res BCR* **2014**;16(3):R47.
 42. Pennington KP, Walsh T, Harrell MI, Lee MK, Pennil CC, Rendi MH, *et al.* Germline and somatic mutations in homologous recombination genes predict platinum response and survival in ovarian, fallopian tube, and peritoneal carcinomas. *Clin Cancer Res* **2014**;20(3):764-75.
 43. de Boer SM, Powell ME, Mileskin L, Katsaros D, Bessette P, Haie-Meder C, *et al.* Adjuvant chemoradiotherapy versus radiotherapy alone for women with high-risk endometrial cancer (PORTEC-3): final results of an international, open-label, multicentre, randomised, phase 3 trial. *Lancet Oncol* **2018**;19(3):295-309.
 44. McMeekin DS, Filiaci VL, Thigpen JT, Gallion HH, Fleming GF, Rodgers WH. The relationship between histology and outcome in advanced and recurrent endometrial cancer patients participating in first-line chemotherapy trials: a Gynecologic Oncology Group study. *Gynecol Oncol* **2007**;106(1):16-22.
 45. Hogberg T, Signorelli M, de Oliveira CF, Fossati R, Lissoni AA, Sorbe B, *et al.* Sequential adjuvant chemotherapy and radiotherapy in endometrial cancer--results from two randomised studies. *Eur J Cancer* **2010**;46(13):2422-31.
 46. Gilks CB, Oliva E, Soslow RA. Poor interobserver reproducibility in the diagnosis of high-grade endometrial carcinoma. *Am J Surg Pathol* **2013**;37(6):874-81.
 47. Mirza MR, Monk BJ, Herrstedt J, Oza AM, Mahner S, Redondo A, *et al.* Niraparib Maintenance Therapy in Platinum-Sensitive, Recurrent Ovarian Cancer. *N Engl J Med* **2016**;375(22):2154-64.
 48. Ledermann J, Harter P, Gourley C, Friedlander M, Vergote I, Rustin G, *et al.* Olaparib maintenance therapy in patients with platinum-sensitive relapsed serous ovarian cancer: a preplanned retrospective analysis of outcomes by BRCA status in a randomised phase 2 trial. *Lancet Oncol* **2014**;15(8):852-61.
 49. Swisher EM, Lin KK, Oza AM, Scott CL, Giordano H, Sun J, *et al.* Rucaparib in relapsed, platinum-sensitive high-grade ovarian carcinoma (ARIEL2 Part 1): an international, multicentre, open-label, phase 2 trial. *Lancet Oncol* **2017**;18(1):75-87.
 50. Gockley AA, Kolin DL, Awtrey CS, Lindeman NI, Matulonis UA, Konstantinopoulos PA. Durable response in a woman with recurrent low-grade endometrioid endometrial cancer and a germline BRCA2 mutation treated with a PARP inhibitor. *Gynecol Oncol* **2018**;150(2):219-226.
 51. Hoppe MM, Sundar R, Tan DSP, Jeyasekharan AD. Biomarkers for Homologous Recombination Deficiency in Cancer. *J Natl Cancer Inst* **2018**; 110(7):704-713.

- 731 52. Mukhopadhyay A, Elattar A, Cerbinskaite A, Wilkinson SJ, Drew Y, Kyle S, *et al.*
732 Development of a functional assay for homologous recombination status in primary
733 cultures of epithelial ovarian tumor and correlation with sensitivity to poly(ADP-
734 ribose) polymerase inhibitors. *Clin Cancer Res* **2010**;16(8):2344-51.
- 735 53. Mukhopadhyay A, Plummer ER, Elattar A, Soohoo S, Uzir B, Quinn JE, *et al.*
736 Clinicopathological features of homologous recombination-deficient epithelial ovarian
737 cancers: sensitivity to PARP inhibitors, platinum, and survival. *Cancer Res*
738 **2012**;72(22):5675-82.
- 739 54. Cruz C, Castroviejo-Bermejo M, Gutierrez-Enriquez S, Llop-Guevara A, Ibrahim YH,
740 Gris-Oliver A, *et al.* RAD51 foci as a functional biomarker of homologous
741 recombination repair and PARP inhibitor resistance in germline BRCA mutated
742 breast cancer. *Ann Oncol* **2018**; 29(5):1203-1210.

743

Table 1: Clinicopathological characteristics stratified for homologous recombination capacity.

	HR deficient	HR proficient	⁷⁴⁴ <i>P</i> value
	n (%)	n (%)	
Total	6 (100)	17 (100)	745
Age, years			
Mean ±SD	70 ±9.3	66 ±10.6	0.431
Tumor			
Primary	6 (100)	17 (100)	
Recurrent	0 (0)	0 (0)	
Histologic subtype			
Endometrioid	0 (0)	11 (65)	0.014^a
Non-endometrioid	6 (100)	6 (35)	
<i>Serous</i>	3 (50)	1 (6)	
<i>Carcinosarcoma</i>	3 (50)	1 (6)	
<i>Clear cell</i>	0 (0)	2 (12)	
<i>Dedifferentiated</i>	0 (0)	2 (12)	
Histologic grade			
1+2	0 (0)	10 (59)	0.019
3	6 (100)	7 (41)	
FIGO 2009			
I	2 (33)	15 (88)	0.021
III/IV	4 (67)	2 (12)	
Adnexal involvement			
yes	1 (17)	2 (12)	1.00
no	5 (83)	15 (88)	
LVSI			
yes	4 (67)	3 (18)	0.045
no	2 (33)	14 (82)	
PTEN-IHC			
loss of expression	1 (17)	8 (47)	0.340
normal expression	5 (83)	9 (53)	
aCGH			
Copy number extremely high	4 (67)	1 (6)	0.019^b
Copy number high	2 (33)	6 (35)	
Copy number low	0 (0)	10 (60)	
TP53			
Mutation	6 (100)	7 (41)	0.019
No mutation	0 (0)	10 (59)	
TCGA subgroups			
<i>TP53</i>	6 (100)	6 (35)	0.014
<i>NSMP/POLE/MMRd</i>	0 (0)	11 (65)	

Bolded *P* values are considered significant ($P < 0.05$). *P* values were calculated using the 2-sided Fisher's exact test for the categorical variables and the unpaired T-test for the difference in age. ^a endometrioid versus non-endometrioid histology was compared. ^b copy number extremely high + copy number high versus copy number low was compared. Abbreviations: LVSI: lymph-vascular space involvement MMRd: mismatch repair deficient, NSMP: no specific molecular profile, SD: Standard deviation, TCGA: Tumor Genome Cancer Atlas.

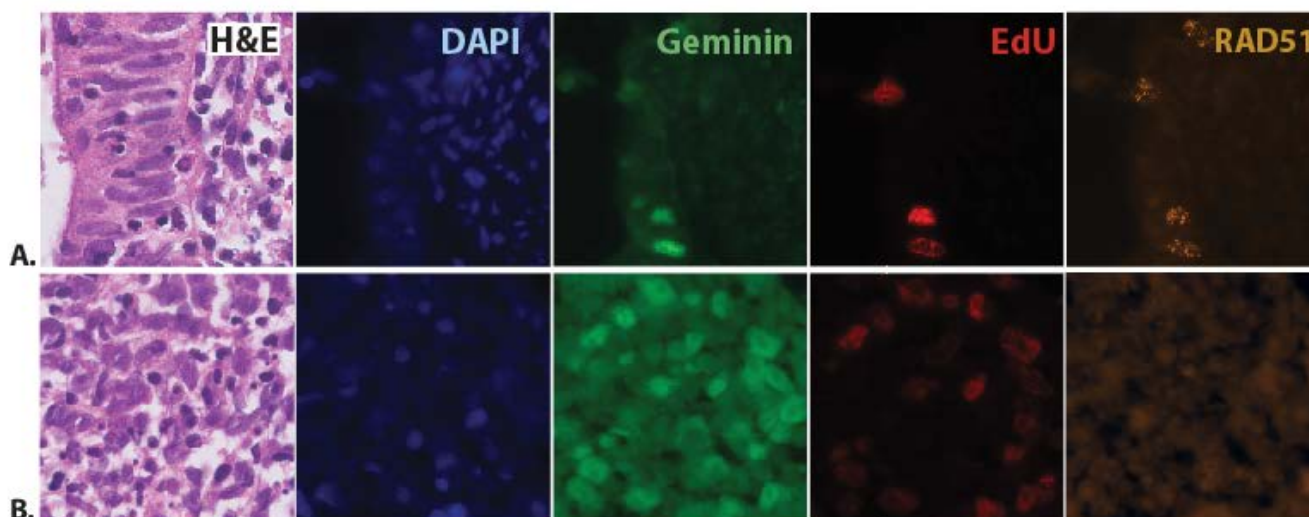


Figure 1: Functional Ex Vivo RAD51-assay to determine homologous recombination repair capacity in EC. A. Example of a homologous recombination repair proficient endometrioid endometrial carcinoma (case 26). In the H&E the presence of tumor tissue is confirmed. Cell nuclei are stained with DAPI. Geminin-staining marks cells in S- and G2-phase. RAD51-foci can be visualized in geminin-positive tumor cells 2 hours after *ex vivo* exposure to X-rays (5 Gy). B. Example of a homologous recombination repair deficient carcinosarcoma (case 13). After *ex vivo* treatment with ionizing radiation, only 2% of the geminin positive cells demonstrates accumulation of RAD51-foci. Abbreviations: EdU: 5-Ethynyl-2'-deoxyuridine, H&E: hematoxylin and eosin.

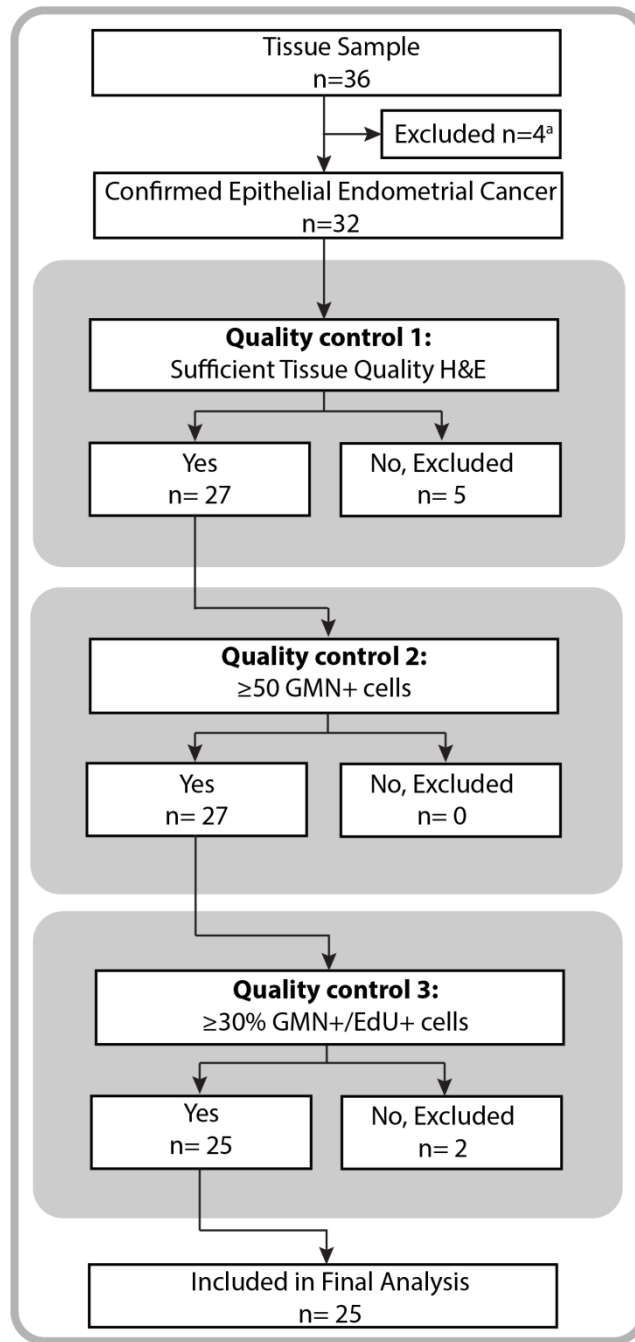


Figure 2: Flow-chart illustrating the selection of cases for analysis. Of 36 samples, four^a cases were excluded because histological evaluation demonstrated no epithelial endometrial malignancy (2x cervical carcinoma, 1x leiomyosarcoma, 1x benign). Tissue was thawed and reanalysed for 10 cases because they did not pass one of the quality controls (QC1; n=5, QC2; n=0, QC3; n=5). For three cases (all initially excluded during QC3), this procedure resulted in sufficient quality improvement to allow inclusion for final analysis. For one case, only frozen tissue was available, which was of sufficient quality. In total, 25 cases passed all quality controls. Abbreviations: QC: quality control, EdU: 5-Ethynyl-2'-deoxyuridine

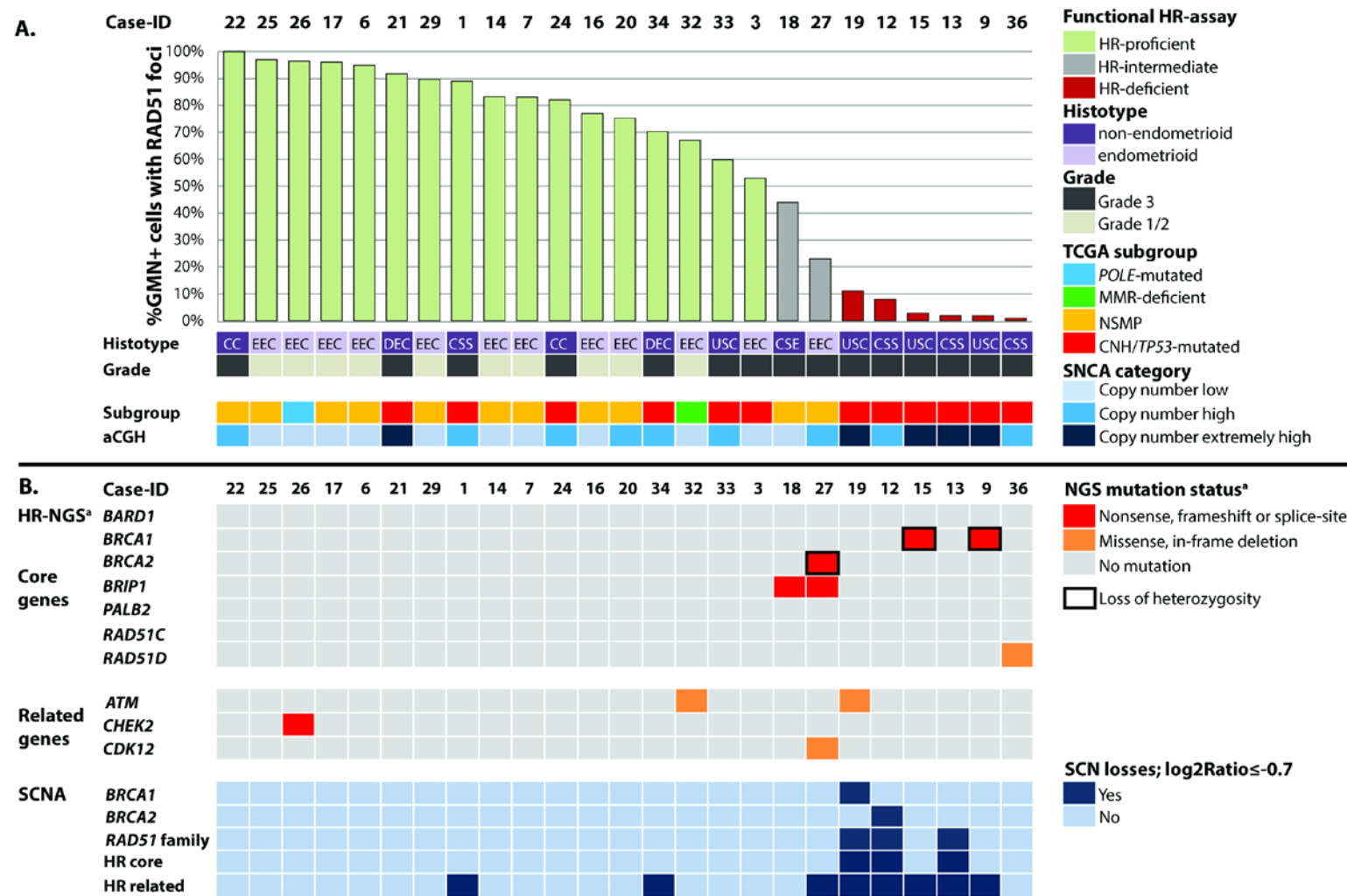


Figure 3: Tumor characteristics (A) and genetic changes (B) stratified for homologous recombination capacity. Each column represents one case. A. Cases were classified in TCGA subgroups using surrogate markers as described in the Supplementary Methods. Case 26 contained a *POLE* variant and a *TP53* variant and was classified in the *POLE*-mutated subgroup. Case 09 demonstrated subclonal loss of *PMS2* with normal expression in the tumor tissue on which the RAD51-assay was performed, together with a *TP53* variant, and was classified as *TP53* mutant. **B.** HR genes were categorized as either being involved in the core process of HR ("core" genes) or being involved in related processes to HR ("related" genes), as previously described by Riaz et al., 2017. **Abbreviations:** CC: Clear Cell Carcinoma, CSE: CarcinoSarcoma with Endometrioid epithelial component, CSS: CarcinoSarcoma with Serous epithelial component, DEC: Dedifferentiated Endometrial Carcinoma, EEC: Endometrioid Endometrial Carcinoma, HR: Homologous Recombination, SCNA: Somatic Copy Number Alterations, TCGA: Tumor Genome Cancer Atlas, USC: Uterine Serous Carcinoma. ^aOnly variants with a variant allele frequency of ≥25% are shown. When multiple variants were present in the same gene, the most pathogenic variant is shown.

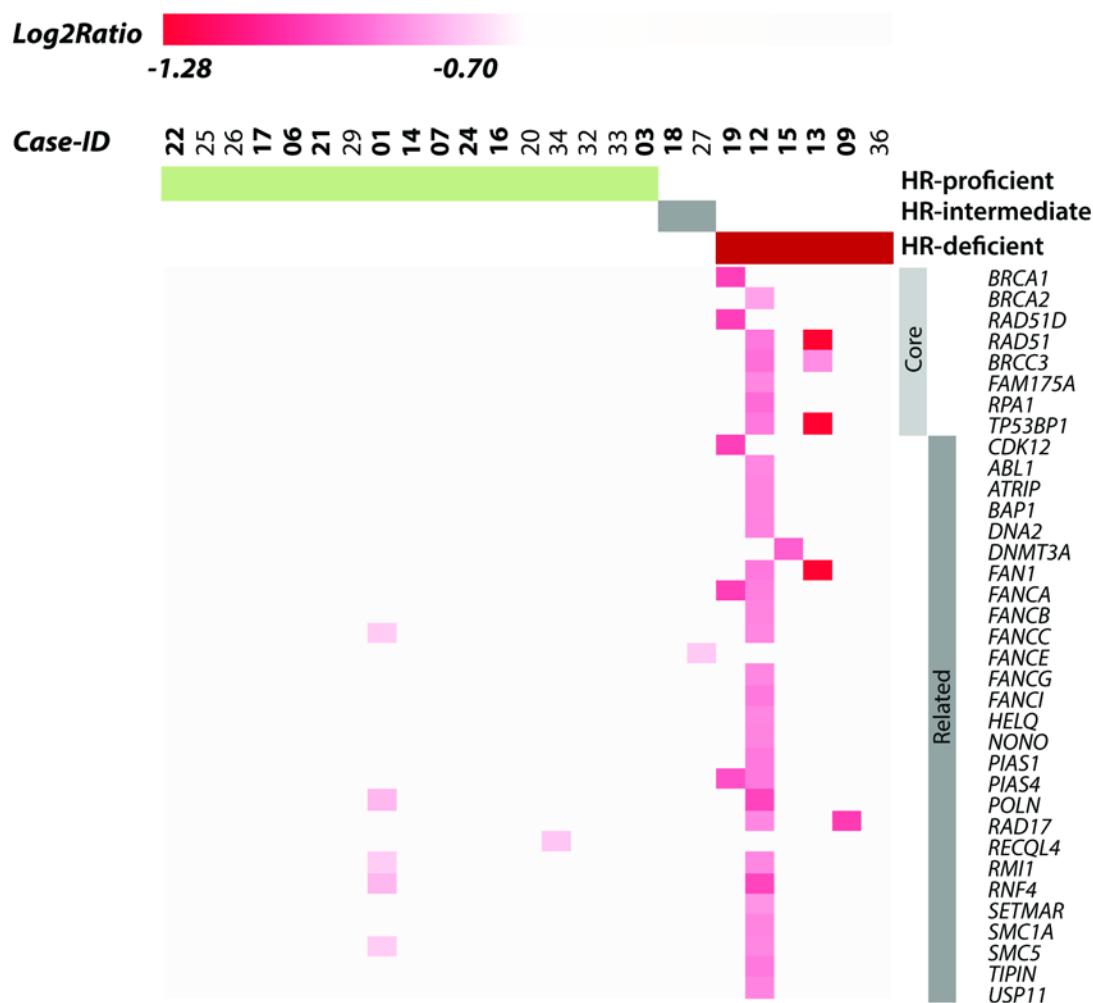


Figure 4: Somatic Copy Number Losses stratified for HR-capacity. Each column represents one case. Homologous recombination (HR) genes were selected and divided in HR-core or HR-related genes as described by Riaz et al, 2017. Only those genes with somatic copy number losses of $\log_2\text{ratio} \leq -0.7$ in at least one of the included cases are visualised. Data were extracted from the aCGH data according to the Supplementary Methods. Bolded cases were analysed using the CGH Agilent platform, others were analysed using the Oncoscan platform.

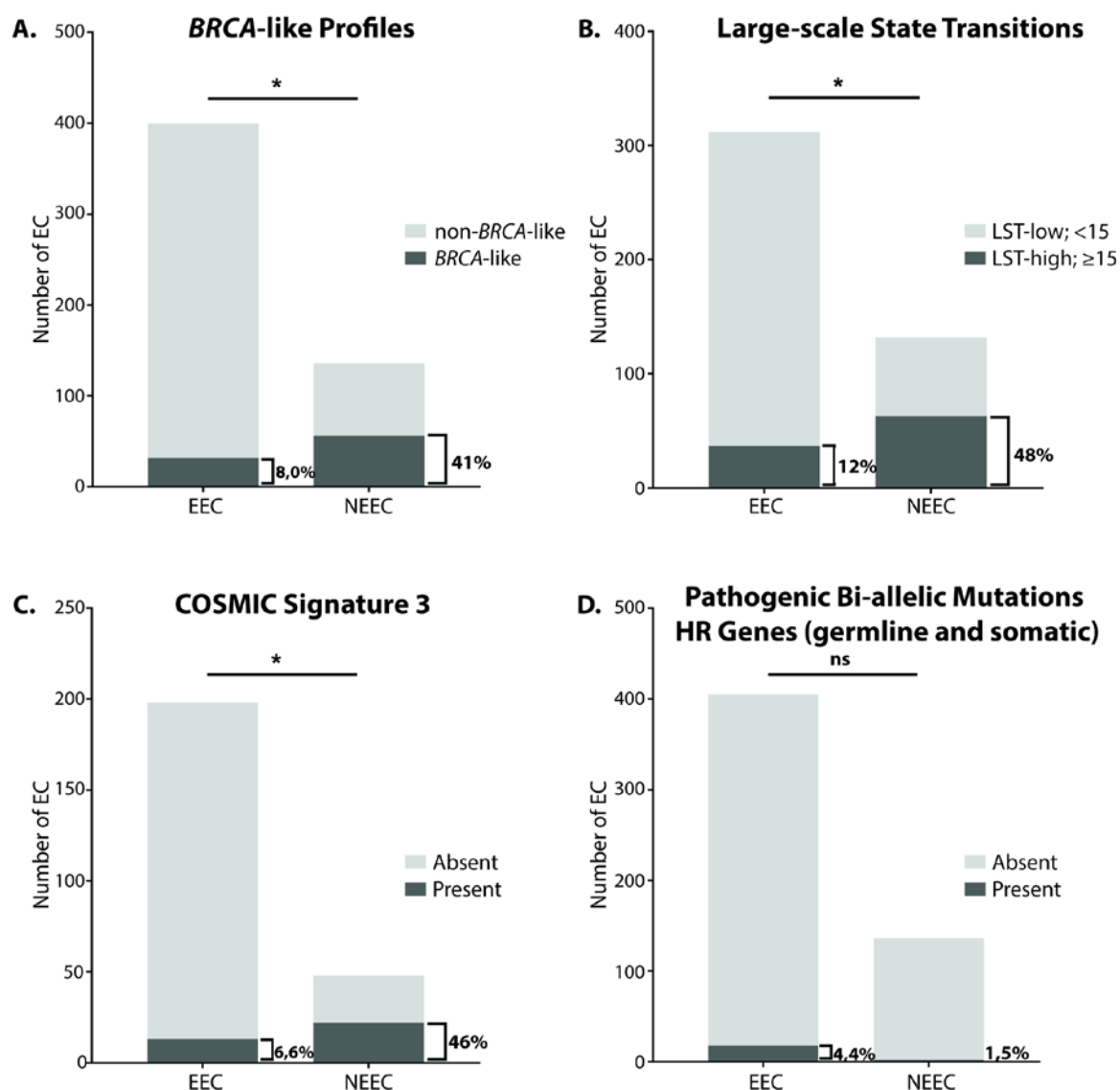
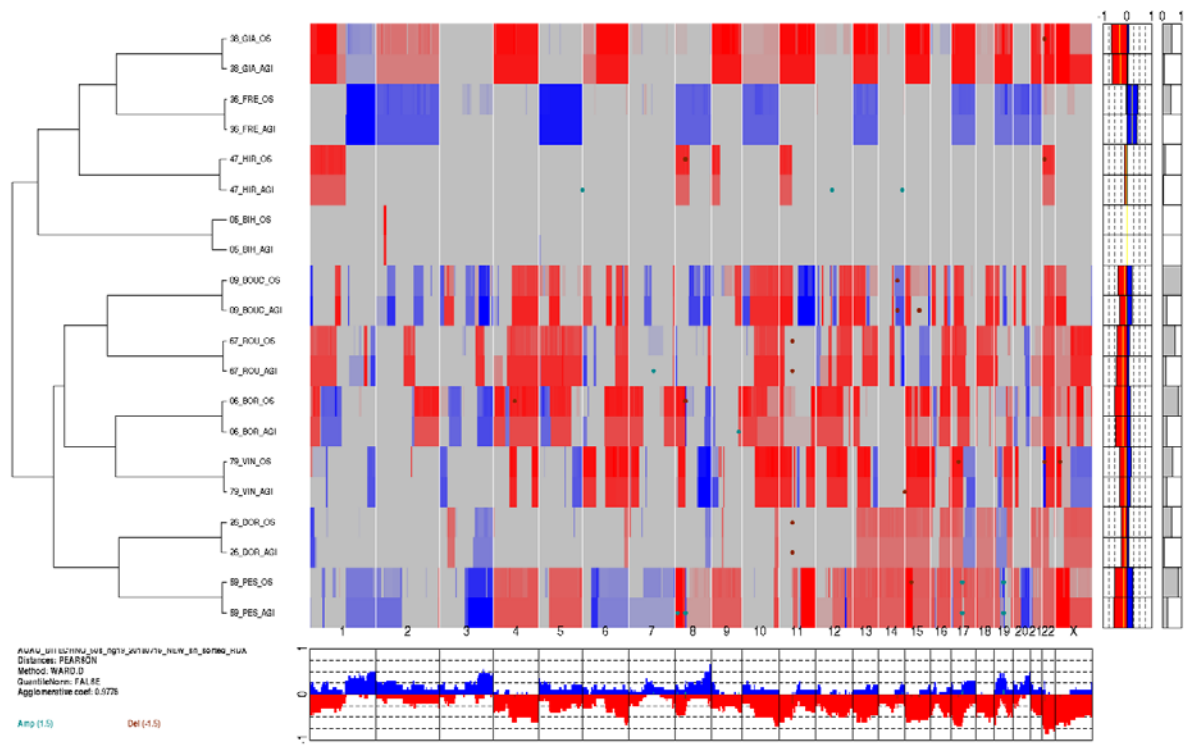
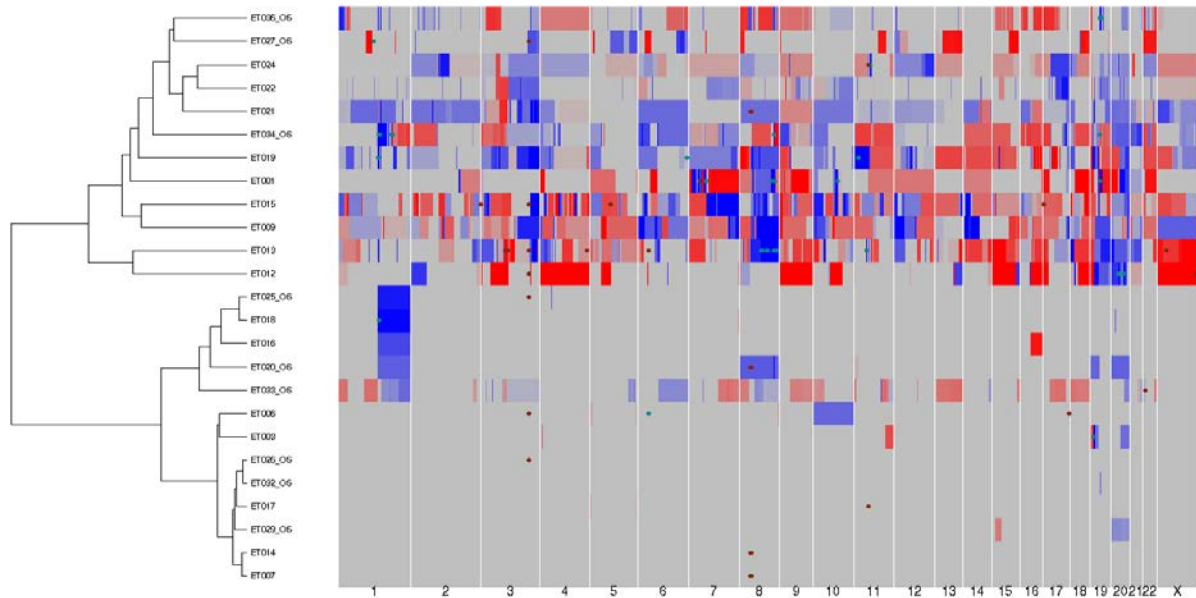


Figure 5: BRCA associated genomic scars as surrogate marker for HR-deficiency in the TCGA-EC cohort. A. A *BRCA*-like profile was present in 32/400 of EEC and 56/136. B. A high LST-score (≥ 15) was present in 37/312 of EEC and 63/132 of NEEC. C. COSMIC signature 3 was present in 13/198 of EEC and 22/48 of NEEC. D. Pathogenic bi-allelic mutations in HR-genes were present in 18/405 of EEC and 2/136 of NEEC. The intertest agreement (accuracy and Cohen's kappa coefficient respectively) were as follows; 0.82 and 0.46 for LST versus *BRCA*-like profiles, 0.84 and 0.40 for LST versus signature 3, 0.85 and 0.36 for *BRCA*-like profiles versus signature 3. Abbreviations: EC: Endometrial Carcinoma, EEC: Endometrioid Endometrial Carcinoma, HRD: Homologous Recombination Deficiency, LST: Large-scale state transitions. ns: not significant. *: $p < 0.001$



Supplementary Figure S1: Unsupervised Euclidean hierarchical clustering on ten paired FFPE and frozen ovarian tumor samples analysed respectively by Oncoscan (OS) or CGH Agilent (AGI) platforms. The figure shows perfect match between paired samples independently from their processing (OS or AGI).



Supplementary Figure S2: Unsupervised Pearson hierarchical clustering on the endometrial tumor samples included in our paper. Samples labelled with “_OS” are those analysed by ONCOSCAN platform, others have been analysed using CGH Agilent technology. As can be seen, there is an unbiased natural division between samples.